

# Fermi-Fermi crossover in the ground state of one-dimensional few-body systems with anomalous three-body interactions

J. R. McKenney and J. E. Drut

*Department of Physics and Astronomy, University of North Carolina, Chapel Hill, North Carolina 27599-3255, USA*



(Received 19 November 2018; published 17 January 2019)

In one spatial dimension, quantum systems with an attractive three-body contact interaction exhibit a scale anomaly. In this work, we examine the few-body sector for up to six particles. We study those systems with a self-consistent, nonperturbative, iterative method in the subspace of zero total momentum. Exploiting the structure of the contact interaction, the method reduces the complexity of obtaining the wave function by three powers of the dimension of the Hilbert space. We present results on the energy, momentum, and spatial structure, as well as Tan's contact. We find a Fermi-Fermi crossover interpolating between large, weakly bound trimers and compact, deeply bound trimers: at weak coupling, the behavior is captured by degenerate perturbation theory; at strong coupling, the system is governed by an effective theory of heavy trimers (plus free particles in the case of asymmetric systems). Additionally, we find that there is no trimer-trimer attraction and therefore no six-body bound state.

DOI: [10.1103/PhysRevA.99.013615](https://doi.org/10.1103/PhysRevA.99.013615)

## I. INTRODUCTION

Quantum gases displaying scale invariance and scale anomalies have been under study both theoretically and experimentally in a variety of contexts in the last two decades. In three dimensions (3D) the unitary Fermi gas is an example of a truly scale invariant, strongly interacting Fermi gas [1,2] (in fact, it displays nonrelativistic conformal invariance [3]), whereas the two-dimensional (2D) version of the same system presents a scale anomaly [4–7]. Both of the above examples have been realized experimentally with ultracold atoms by several groups, and in particular, the 2D case has been under intense scrutiny in recent years (see, e.g., [8–18]). The effect of the anomaly in 2D has also been extensively studied from the theoretical side (see, e.g., [19–27], and [28] for a review).

In the recent work of Ref. [29], it was shown that a very simple generalization of the 2D scale-anomalous Fermi gas mentioned above can be achieved in one dimension (1D) as well. There, a three-species system of fermions, with an interaction fine tuned such that only three-body forces are present, contains a dimensionless coupling constant that induces a bound state (trimer) at arbitrarily small couplings. At about the same time, the bosonic analog was studied by several groups in Refs. [30–33], where the few- to many-body properties were explored both analytically and numerically. In particular, such bosons were shown to form many-body bound states (“droplets” [33]) whose energy grows faster than exponentially with the particle number.

In contrast to the bosonic case mentioned above, relatively little is known about fermions. For instance, Ref. [29] only addressed the fully symmetric three-body problem (i.e., the  $1 + 1 + 1$  problem) and left open the questions of whether two fermionic trimers are attractive or repulsive (which would presumably leave an imprint on the nature of the many-body ground state), and whether there is a coupling-dependent crossover in the many-body behavior.

These types of questions are also relevant from a more general perspective, as three-body forces play a central role in nuclear physics. Indeed, two-body forces are typically regarded as the most important feature of interacting models, but three-body forces are being acknowledged as increasingly relevant [34].

In this work, we seek to address the properties of few-body, fermionic systems with three-body contact interactions in 1D. Because the Pauli exclusion principle prohibits contact interactions between two fermions of the same flavor, the minimum nontrivial number of fermionic components for this model is three, which we employ. Although it is likely a challenge to engineer three-body forces, multiflavor experiments with  $SU(N)$  symmetry have been underway for a few years [35], in particular, for  $N = 3$  [36–38]. Here, we investigate specifically the energetics and structure of all possible interacting cases with up to six particles, labeling them by the numbers of fermions of each component, e.g.,  $2 + 2 + 2$  indicates two fermions of each flavor.

Conventionally, 1D few- and many-fermion problems can be solved exactly by way of the Bethe ansatz. The presence of three-body interactions, however, makes this problem effectively 2D when particles approach the interaction region, as we showed in Ref. [29] (see also below). As a consequence, the problem addressed here requires a different kind of computational method. Fortunately, contact interactions allow for simplifications which, as we will show below, make few-body problems tractable for up to six particles with modest computational resources. For those cases, the full wave function is, in fact, accessible.

Our approach bears conceptual similarities to the Faddeev-Yakubovsky equations [39], where the wave function is separated into interacting and noninteracting pieces, as well as to the Skorniakov–Ter Martirosian equations [40], where a three-body problem is reduced to a lower-dimensional integral

equation. Our method is also reminiscent of the Lippmann-Schwinger equation [41].

The remainder of the paper is organized as follows: In Sec. II, we describe the Hamiltonian of the model, provide an example of the simplest case, and explain how the coupling is renormalized. Section III introduces our computational method at length and provides details about the numerical implementation. Results obtained are presented in Sec. IV, and we summarize and conclude in Sec. V.

## II. HAMILTONIAN AND RENORMALIZATION

The system is defined by the following Hamiltonian:

$$\hat{H} = \sum_{s=1,2,3} \int dp \epsilon(p) \hat{a}_{s,p}^\dagger \hat{a}_{s,p} + g \int dx \hat{n}_1(x) \hat{n}_2(x) \hat{n}_3(x), \quad (1)$$

where  $\epsilon(p) = \frac{\hbar^2 p^2}{2m}$ . Here,  $\hat{a}_{s,p}^\dagger$  and  $\hat{a}_{s,p}$  are the fermionic creation and annihilation operators for particles of species  $s$  and momentum  $p$ , and  $\hat{n}_s(x)$  is the corresponding density at position  $x$ . Throughout this work, we will take  $\hbar = k_B = m = 1$ .

In what follows, we use the momentum (position) variables  $p, k, q$  (respectively  $x, y, z$ ) to distinguish between fermionic species. For instance, in first quantization, the Hamiltonian for the four-body  $2 + 1 + 1$  system is

$$\hat{H} = \frac{1}{2} (\hat{p}_1^2 + \hat{p}_2^2 + \hat{k}^2 + \hat{q}^2) + g \sum_{i=1}^2 \delta(x_i - y) \delta(y - z). \quad (2)$$

For other numbers of particles, one interaction term must be included for every possible combination of three different-flavored fermions (trimers). Fermions of the same species do not interact because of the Pauli exclusion principle.

In order to renormalize the bare coupling  $g$ , we choose a lattice regularization such that from this point on the bare coupling  $g$  is a lattice coupling. The connection between  $g$  and the specific physical situation is determined by a renormalization prescription which relates  $g$  to the lattice momentum cutoff  $\Lambda$  and the trimer binding energy  $\epsilon_B$ . That relationship is obtained by solving the three-body problem as shown in Ref. [29], which yields

$$\frac{1}{g} = -\frac{1}{L^2} \sum_{\mathbf{k}} \frac{1}{\epsilon_{\mathbf{k}} + \epsilon_B}, \quad (3)$$

where  $L = N_x \ell$  is the lattice size,  $\ell$  is the lattice spacing,  $\epsilon_{\mathbf{k}} = (k_1^2 + k_2^2 + k_3^2)/2$ ,  $\mathbf{k} = (2\pi/L)(n_1, n_2, n_3)$ , and the sum covers  $0 \leq |n_1 + n_2| \leq \Lambda$ , with the constraint  $n_1 + n_2 + n_3 = 0$  (i.e., vanishing total momentum).

As can be appreciated in Eq. (3), the ultraviolet (i.e., short-range) behavior of the momentum sum is the same as that of the 2D two-body problem in the sense that they both diverge logarithmically [29]. We thus see that even though our problem is in 1D globally, it is in 2D locally.

## III. FORMALISM

As mentioned above, in this work we consider systems with three species of fermions 1,2,3 and corresponding vary-

ing particle numbers  $N_1, N_2, N_3$ . We will fix those numbers and refer to the corresponding system as the  $N_1 + N_2 + N_3$  problem. As species 1,2,3 are distinguishable from one another but particles are otherwise identical, we use as a starting point a product wave function with one factor for each species, i.e., we start with a multiparticle wave function of the form  $\psi = \psi_1 \psi_2 \psi_3$ .

Within a given species, the wave function must be antisymmetric with respect to particle exchange, and to impose that property we expand that factor in a basis of Slater determinants of plane waves. (In particular, we use a single Slater determinant as a starting point in the iteration process described below.) Since the Hamiltonian preserves particle symmetry and the symmetric and antisymmetric subspaces are orthogonal, this initial projection is sufficient to capture the antisymmetry of the true wave function of the interacting system. In particular, when transforming from the position-space wave function  $\psi(\mathbf{x})$  to the momentum-space wave function  $\phi(\mathbf{p})$ , the usual (unsymmetrized) Fourier transform may be used. Additionally, we make use of the fact that the total momentum is conserved and impose a zero-total-momentum constraint on the multiparticle wave function.

Formally, our approach consists in separating the kinetic and potential energy operators and grouping the former with the energy eigenvalue  $E$  in the Schrödinger equation, i.e., if  $\hat{H} = \hat{T} + \hat{V}$ , then we write the eigenvalue problem as

$$\phi = \frac{1}{\hat{T} - E} \hat{V} \phi, \quad (4)$$

where  $\phi$  is the multiparticle wave function and the inverse of  $\hat{T} - E$  is easily addressed as it is diagonal in momentum space. The problem now becomes that of finding, for a proposed  $E$ , whether such a unit-eigenvalue equation can be satisfied. To that end, we implement the iterative approach described below which, crucially, exploits the zero-range nature of the interaction to avoid computing determinants (which would be the conventional way to solve the above problem).

As an illustration, consider the simplest nontrivial case of  $2 + 1 + 1$  particles. The kinetic energy terms are simply given by the sum of the kinetic energies of the individual particles. As shown in Eq. (2), the interacting part of the Schrödinger equation contains two terms corresponding to the two different ways in which the  $1 + 1$  subsystem can interact with the two identical particles. We consider just one of those terms and proceed in momentum space.

One of the identical particles is a spectator, while the other three interact such that the Fourier transform over the former is trivial. As usual, translation invariance yields a  $\delta$  function that imposes conservation of total momentum of the reactants, leading to

$$\frac{g}{L^2} \sum_{p'_1, k', q'} \phi(p'_1, p_2, k', q') \delta(P_1 - P'_1), \quad (5)$$

where  $P_1 = p_1 + k + q$  and  $P'_1 = p'_1 + k' + q'$ . While explicitly a function of all four momentum variables, this term can be reduced to a function of only one by choosing the center-of-momentum frame (i.e., only eigenstates of the total momentum operator with eigenvalue zero are considered), such that  $P_1 + p_2 = 0$ ; from here on out, we will work in this

frame. Then the  $\delta$  function appears as  $\delta(P_1' + p_2)$ . Including both contributions to the interacting piece and rearranging, the full Schrödinger equation becomes

$$\phi(p_1, p_2, k, q) = G_0(P^2) \sum_i (-1)^i f(p_i), \quad (6)$$

where the fermionic antisymmetry is manifest. Here  $P^2 = \frac{1}{2}(p_1^2 + p_2^2 + k^2 + q^2)$  is the total kinetic energy, and

$$G_0(P^2) = \frac{-g/L^2}{P^2 - E} \quad (7)$$

is the noninteracting propagator multiplied by  $-g/L^2$ . The function  $f$ , not yet determined, is related to  $\phi$  by

$$f(p) = \frac{1}{2!} \sum_{u,v} (1 - \hat{P}_{up}) \phi(u, p, v, \varsigma), \quad (8)$$

where  $u, v$  are dummy variables, and the first sum has been carried out using the  $\delta$  function; the operator  $\hat{P}_{up}$  exchanges  $u$  and  $p$ . Here and in what follows,  $\varsigma$  denotes the negative of the sum of all other momentum variables present as arguments, which results from momentum conservation; thus, in the above equation,  $\varsigma = -u - p - v$ .

The benefit of this approach is apparent already in Eq. (6) upon considering the indistinguishability of fermions of the same species. Indeed, together with zero total momentum and the freedom to relabel summation indices, all interaction terms were brought into the same functional form using the function  $f(p)$  of Eq. (8), which depends on only one momentum variable.

By substituting Eq. (6) into Eq. (8), an implicit summation equation for  $f$  is obtained which can be solved iteratively. Being a function of only one variable instead of four,  $f$  is much more amenable to an iterative solution than the original equation in terms of the momentum-space wave function  $\phi$ . This three-dimensional reduction in the complexity of the problem that must be solved is a general feature of this method for the three-body contact interaction.

TABLE I. Wave functions and auxiliary functions for various systems. The collective index  $(p_1 p_2 u)$ , appearing in sums in the third column, indicates a summation over cyclic permutations of  $p_1, p_2, u$  as the first three arguments of  $\phi$ , which correspond to like-flavor fermions. All  $f$  expressions are summed over  $u$  and  $v$ . The argument of  $G_0(P^2)$  is always the sum of the kinetic energies of all the particles in the system, i.e.,  $P^2 = \frac{1}{2}(\sum_i p_i^2 + \sum_j k_j^2 + \sum_k q_k^2)$ .

System	$\phi$	$f$ Summand	Normalization summand
2+1+1	$G_0 \sum_i (-1)^i f(p_i)$	$\frac{1}{2!} (1 - \hat{P}_{up}) \phi(u, p, v, \varsigma)$	$G_0^2 f(p_1) \sum_i (-1)^{i+1} f(p_i)$
2+2+1	$G_0 \sum_{i,j} (-1)^{i+j} f(p_i, k_j)$	$\frac{1}{(2!)^2} (1 - \hat{P}_{up})(1 - \hat{P}_{vk}) \phi(u, p, v, k, \varsigma)$	$G_0^2 f(p_1, k_1) \sum_{i,j} (-1)^{i+j} f(p_i, k_j)$
3+1+1	$G_0 \sum_{i,j,k} \epsilon_{ijk} f(p_i, p_j)$	$\frac{1}{3!} \sum_{(p_1 p_2 u)} \phi(p_1, p_2, u, v, \varsigma)$	$G_0^2 f(p_1, p_2) \sum_{i,j,k} \epsilon_{ijk} f(p_i, p_j)$
2+2+2	$G_0 \sum_{i,j,k} (-1)^{i+j+k} f(p_i, k_j, q_k)$	$\frac{1}{(2!)^3} (1 - \hat{P}_{up})(1 - \hat{P}_{vk_1}) \times (1 - \hat{P}_{\varsigma q_1}) \phi(u, p_1, v, k_1, \varsigma, q_1)$	$G_0^2 f(p_1, k_1, q_1) \sum_{i,j,k} (-1)^{i+j+k+1} f(p_i, k_j, q_k)$
3+2+1	$G_0 \sum_{i,j,k,l} (-1)^l \epsilon_{ijk} f(p_i, p_j, k_l)$	$\frac{1}{3! \cdot 2!} \sum_{(p_1 p_2 u)} (1 - \hat{P}_{vk_1}) \phi(u, p_1, p_2, v, k_1, \varsigma)$	$G_0^2 f(p_1, p_2, k_1) \sum_{i,j,k,l} (-1)^{l+1} \epsilon_{ijk} f(p_i, p_j, k_l)$
4+1+1	$G_0 \sum_{i,j,k,l} \epsilon_{ijkl} f(p_j, p_k, p_l)$	$\frac{1}{4!} \{1 - [1 - (1 - \hat{P}_{up_3}) \hat{P}_{up_2}] \hat{P}_{up_1}\} \times \phi(u, p_1, p_2, p_3, v, \varsigma)$	$G_0^2 f(p_1, p_2, p_3) \sum_{i,j,k,l} \epsilon_{ijkl} f(p_i, p_j, p_k)$

Up to this point, the energy eigenvalues have not been addressed. By requiring the momentum-space wave function  $\phi$  to be normalized, however, we obtain an equation that, when solved simultaneously with the aforementioned summation equation for  $f$ , fixes  $E$ . A further simplification arises here: Since all momenta are summed over, particle species are interchangeable in  $f$  inside the sums, greatly reducing the number of terms. Finally,  $\phi$  (and  $f$ ) may be taken to be real, since any imaginary part would obey the same equation. All told, the normalization condition which fixes  $E$  is

$$1 = \sum_{p_1, p_2, k, q} G_0^2(P^2) f(p_1) \sum_i (-1)^{i+1} f(p_i), \quad (9)$$

where constant prefactors have been omitted for reasons discussed in the next section. With periodic boundary conditions, the kinetic contributions are expanded as  $(\frac{2\pi n}{L})^2$ ,  $n$  integer, and the energy is expressed in terms of the three-body energy as  $-E = \alpha \epsilon_B$ , where  $\epsilon_B$  is the (positive) binding energy of the trimer at the given coupling.

The different five- and six-body systems can be treated in a similar fashion; the corresponding expressions for all possible interacting configurations are collected in Table I. In all cases, when constructing the definition of  $f$ , it is crucial to do so in a way that retains the ordering of like-flavor fermions as arguments of  $\phi$ .

### A. Iterative method

For all cases, the wave function  $\phi$  is initialized as a uniform momentum distribution subject to the constraints of antisymmetrization and zero total momentum. The auxiliary functions  $f$  are constructed from such  $\phi$  (see Table I, third column) before being fed into their defining implicit equations (see Table I, second and third columns). An initial run of 4000 iterations on  $f$  is carried out before continuing until the lowest energy value of  $\alpha = -E/\epsilon_B$  that leads to a properly normalized wave function (built from  $f$ ) is converged to a tolerance of  $10^{-3}$ . The numerical value of  $\alpha$  is determined

by cubic spline interpolation of the normalization of  $\phi$  in a monotonic neighborhood containing unity.

To ensure numerical stability,  $f$  is divided by the most recent normalization of  $\phi$  before each iteration. Since the implicit summation equation is unaffected by overall factors (by virtue of the fact that the Schrödinger equation is linear), this division has no impact on the functional form; thus, constant prefactors, including those proportional to  $g/L^2$  and those arising from combinatorics, are absorbed into the overall scale of  $f$  and thus may be omitted from the normalization expressions. (All coupling dependence is carried and enforced by the implicit equation for  $f$ .) While all values of  $\alpha$  of course lead to proper normalizations immediately after this step, only the correct  $\alpha$  is a fixed point and remains equal to unity after repeated iterations. While the outermost momentum loops are carried out in parallel, all other entries of  $f$  are updated as soon as they are computed, as in the Gauss-Seidel method.

### B. Weak-coupling expansion

In the limit of very small coupling, we expect that the ground state can be expressed as a linear combination of noninteracting ground states. In this limit, the energy can be written as  $E = E_{FG} - \epsilon$ , where  $E_{FG}$  is the energy of the noninteracting free gas (FG) ground state and  $\epsilon$  is a small deviation of the order of  $\epsilon_B$ . At leading order in  $\epsilon$ , the surviving terms in the sum over  $G_0(P^2)$  are the ones for which  $P^2 = E_{FG}$ . Similarly, at leading order in  $\epsilon_B$ ,  $-g/L^2 \approx \epsilon_B$ . As a result,

$$G_0(P^2) = \frac{\epsilon_B}{\epsilon} + O\left(\frac{\epsilon_B}{P^2}\right). \quad (10)$$

Working in the basis of noninteracting FG states, the momentum sums appearing in the equations for  $f$  may now be carried out in closed form, allowing an exact solution at weak coupling.

## IV. RESULTS

Using the technique described above, we have explored the properties of all attractively interacting systems with up to six particles beyond the already solved case of three particles (namely, the  $1 + 1 + 1$  problem): four particles ( $2 + 1 + 1$ ); five particles ( $2 + 2 + 1$  and  $3 + 1 + 1$ ); and six particles ( $2 + 2 + 2$ ,  $3 + 2 + 1$ , and  $4 + 1 + 1$ ). In this section we show, for those systems, our results for the ground-state energy, spatial and momentum structure, and Tan's contact of all six systems across five orders of magnitude in the trimer binding energy  $\epsilon_B$  [expressed in dimensionless form as  $\epsilon_B \equiv (2\pi/L)^{-2}\epsilon_B$ ].

### A. Energy

Figure 1 shows our results for the ground-state energy  $E$  of the various few-body problems as a function of the binding energy  $\epsilon_B \equiv (2\pi/L)^{-2}\epsilon_B$  of the trimer.  $E_{FG}$  is the ground-state energy of the corresponding noninteracting system, and  $N = N_1 + N_2 + N_3$  is the total particle number. In all cases, the energy of the system is progressively more dominated by the binding energy of the trimer as the coupling is increased.

At weak coupling, one may attempt to capture the physics of the system with perturbation theory, which amounts to computing  $\langle \hat{V} \rangle$  in a noninteracting ground state, where  $\hat{V}$  is the three-body interaction. As we will show, however, the

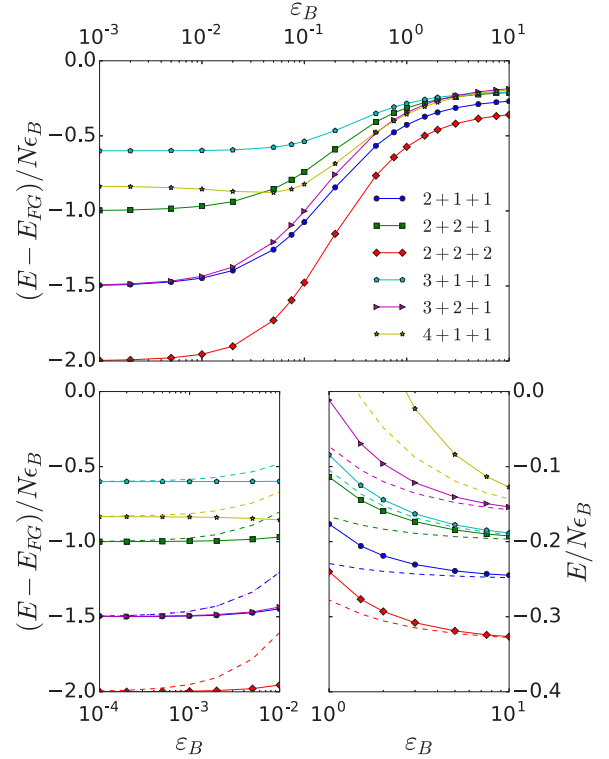


FIG. 1. Top: Ground-state energy  $E$  per particle of few-body systems as a function of the coupling, as measured by the binding energy  $\epsilon_B \equiv (2\pi/L)^{-2}\epsilon_B$  of the trimer.  $E_{FG}$  is the ground-state energy of the corresponding noninteracting system. (Bottom left) Weak-coupling regime, where dashed lines depict the NLO perturbative approximation using a linear combination of noninteracting ground states. (Bottom right) Energy per particle at strong coupling in units of the trimer binding energy; the limiting values in this case are given by the number of trimers formed, divided by  $N$ , which yields (from bottom to top)  $-1/3$ ,  $-1/4$ ,  $-1/5$ ,  $-1/5$ ,  $-1/6$ , and  $-1/6$ . Dashed curves depict the NLO approximation in the particle-to-trimer mass ratio with Bethe-Peierls boundary conditions.

interaction term breaks the degeneracy among noninteracting ground states; carrying out that calculation using a valid, but arbitrary, noninteracting ground state would not yield the correct result. Instead (using a linear combination of noninteracting ground states), degenerate perturbation theory at next-to-leading order (NLO) yields the dashed lines of Fig. 1 (bottom left), which agree with our nonperturbative results in the weak-coupling limit. Our nonperturbative calculation converges to the following values (from bottom to top):  $-2$  (red),  $-3/2$  (blue, magenta),  $-1$  (green),  $-5/6$  (yellow), and  $-3/5$  (cyan). The NLO energy of a single trimer would appear in all the panels of Fig. 1 simply as  $-1/3$ , which is actually (and deceptively) the exact result at all couplings.

To find the correct linear combinations of noninteracting ground states, we may solve the equations for  $f$  at weak coupling as described previously. For the  $2 + 1 + 1$  system, the FG states allow only momentum values of  $p = 0$  and  $|p| = 1$ , allowing us to write

$$\begin{pmatrix} 3 & -2 & -1 \\ -2 & 4 & -2 \\ -1 & -2 & 3 \end{pmatrix} \begin{pmatrix} f(-1) \\ f(0) \\ f(1) \end{pmatrix} = \frac{\epsilon}{\epsilon_B} \begin{pmatrix} f(-1) \\ f(0) \\ f(1) \end{pmatrix}, \quad (11)$$

yielding eigenvalues of  $\epsilon = 4\epsilon_B$  and  $\epsilon = 6\epsilon_B$ , where the total energy is  $E = E_{FG} - \epsilon$ ; there is also a spurious solution of  $\epsilon = 0$  that is inconsistent with the assumed approximation. This splitting of energies demonstrates how an arbitrarily small coupling breaks the degeneracy of the FG states. The eigenvector corresponding to the ground state,  $\epsilon = 6\epsilon_B$ , demands that  $f(-1) = f(1) = -\frac{1}{2}f(0)$ . Consistency with the equations in Table I then determines

$$f(p) = \sqrt{2}[\delta(p-1) - 2\delta(p) + \delta(p+1)], \quad (12)$$

which also allows determination of the position-space wave function as

$$\psi(x_1, x_2, y, z) = \tilde{\psi}(x_2, y, z) - \tilde{\psi}(x_1, y, z), \quad (13)$$

where  $\tilde{\psi}(x, y, z) = \frac{1}{\sqrt{2}L^2} [\cos(\frac{2\pi(x-y)}{L}) + \cos(\frac{2\pi(x-z)}{L})]$ . The same procedure may be carried out for the other systems; in all cases, the ground-state eigenvalues agree with the limiting values in Fig. 1 (bottom left).

In the limit of strong coupling, trimers will be extremely localized and act as impenetrable, composite fermions. The low-energy effective Hamiltonian in terms of noninteracting trimers and the remaining unbound fermions can be written as

$$\hat{H}_{\text{eff}} = \frac{1}{2m} (\hat{p}_{\text{unbound}}^2 + \lambda \hat{p}_{\text{trimer}}^2), \quad (14)$$

where  $\lambda = 1/3$  is the fermion-to-trimer mass ratio and is treated as a small parameter. For all of the systems considered here except the  $2+2+2$  problem, only one trimer forms. In those cases, the limit of small  $\lambda$  yields a massive trimer which, using Bethe-Peierls boundary conditions, shows that the problem is equivalent to that of noninteracting fermions in a 1D hardwall box. Using that mapping, we present results on a NLO (first order in  $\lambda$ ) approximation to the energy for comparison with our numerical results in Fig. 1 (bottom right), for which we find the agreement to be excellent. The  $2+2+2$  system comprises two trimers, so we treat its strong-coupling limit as that of two identical fermions of mass  $3m$  on a 1D ring; again, the agreement is very satisfactory.

### B. Trimer-trimer interaction and (un-)bound state

Of particular interest is the nature of the interaction between two trimers. At strong coupling, the deeply bound trimers likely repel each other due to Pauli exclusion of their constituent fermions. At weak and intermediate couplings, however, it is *a priori* possible for the trimer-trimer interaction to be attractive, such that hexamers may form, and that trimer-trimer pairing may affect the nature of the ground state in the many-body regime.

To address this question, we apply our method to the  $2+2+2$  system, fixing the energy to twice the binding energy  $\epsilon_B$  (the threshold for attractive interaction), and search for the smallest value of  $\epsilon_B$  that allows a normalized wave function. While this can be carried out numerically, our results indicate that such a hexamer state is not physical. In Fig. 2, the calculated energy of this state is larger than the kinetic energy associated with the momentum cutoff  $\Lambda$ , violating the necessary separation of scales in our renormalization scheme. Furthermore, in contrast to all other cases investigated, the energy does not converge to a continuum value in the limit of large  $N_x$ . Combined with the fact that the  $2+2+2$  system's

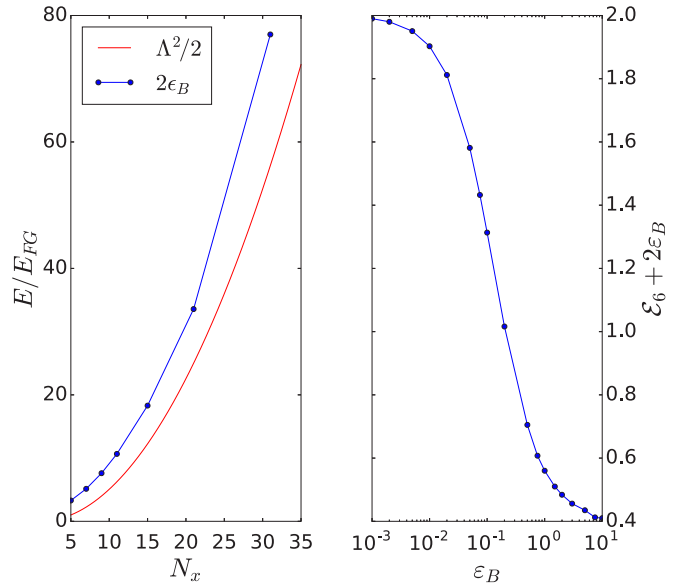


FIG. 2. (Left) Coupling ( $\epsilon_B$ ) required for threshold trimer-trimer binding. In addition to diverging in the continuum limit, the energy of the bound hexamer state (dotted blue) always exceeds the lattice cutoff energy (red), indicating that no such state exists. (Right) Energy of the  $2+2+2$  system relative to the energy of two trimers, showing that the trimers repel each other.

energy appears to approach  $2\epsilon_B$  asymptotically from below (see Tables II and III), we conclude that the trimers approach a hard-core repulsive interaction in the limit of large coupling.

Based on the above analysis, we conclude that at least at the few-body level there is no trimer-trimer bound-state formation. It remains to be determined whether the presence of a Fermi surface (i.e., a finite background fermion density) induces trimer-trimer pairing in the many-body regime.

## C. Structure

### 1. Momentum structure

In Figs. 3 and 4 we show the momentum distribution for the  $2+1+1$  problem at weak and strong coupling, respectively. As expected, at weak coupling, only low-lying momentum states are occupied. As we increase the coupling, higher momentum states become filled (Fig. 4; note the difference in scales compared to Fig. 3). We anticipate that the increased number of momentum states contributing at strong coupling corresponds to enhanced spatial localization of trimers.

### 2. Spatial structure: Selected two-body density matrices

Since  $f$  provides full information on the momentum-space wave function, we can also access the position-space wave function by Fourier transformation. Here we provide spatial density distributions of the simplest case ( $2+1+1$ ) to illustrate how an excess particle positions itself around a trimer. In Figs. 5 and 6, we present the particle density of the two identical particles as a function of their positions. Since the system is translation invariant, we fix the position of one of the unique fermions at the origin and integrate over the position of the other. With this choice, the (1D) origin serves as the center of the trimer and we will refer to it accordingly.

TABLE II. Numerical energy ratios  $\alpha = -E/\epsilon_B$  corresponding to each coupling  $\epsilon_B = (2\pi/L)^{-2}\epsilon_B$ .

$\epsilon_B$	System					
	2 + 1 + 1	2 + 2 + 1	3 + 1 + 1	2 + 2 + 2	3 + 2 + 1	4 + 1 + 1
$10^{-3}$	-994.019	-995.016	-997.001	-1988.024	-1991.045	-3994.985
$2 \times 10^{-3}$	-494.038	-495.031	-497.002	-988.048	-991.085	-1994.970
$5 \times 10^{-3}$	-194.107	-195.078	-197.004	-388.126	-391.193	-794.929
$10^{-2}$	-94.208	-95.154	-97.011	-188.269	-191.385	-394.869
$2 \times 10^{-2}$	-44.411	-45.306	-47.030	-88.589	-91.757	-194.779
$5 \times 10^{-2}$	-14.969	-15.729	-17.117	-29.626	-32.751	-74.736
$7.5 \times 10^{-2}$	-8.698	-9.369	-10.546	-17.097	-20.096	-48.202
$10^{-1}$	-5.702	-6.301	-7.313	-11.133	-13.989	-35.067
$2 \times 10^{-1}$	-1.626	-2.045	-2.673	-3.081	-5.453	-15.888
$5 \times 10^{-1}$	0.264	0.036	-0.246	0.590	-1.116	-5.144
$7.5 \times 10^{-1}$	0.573	0.403	0.209	1.190	-0.306	-2.925
1	0.706	0.569	0.422	1.440	0.068	-1.864
1.5	0.823	0.724	0.625	1.660	0.417	-0.837
2	0.875	0.797	0.721	1.758	0.577	-0.341
3	0.922	0.867	0.815	1.848	0.729	0.137
5	0.956	0.922	0.888	1.913	0.843	0.503
7.5	0.972	0.949	0.924	1.945	0.896	0.680
10	0.979	0.962	0.942	1.959	0.923	0.764

Figure 5 shows the analytical results in the weakly interacting limit (our nonperturbative result at  $\epsilon_B = 10^{-4}$  is indistinguishable from the perturbative result at  $\epsilon = 6\epsilon_B$ ). The left panel reveals that the ground state favors a configuration of one large trimer far away from a free particle. The first excited state, however, favors a four-body molecular configuration (right panel) where the two identical fermions are equidistant from the molecular center. The probability distribution,

$$P(|x_2 - x_1|/L) = \int dy dz |\psi(x_1, x_2, y, z)|^2, \quad (15)$$

for particle separations  $|x_2 - x_1|$  is plotted in Fig. 7, showing that the ground state typically maximizes the distance between identical fermions.

Figure 6 provides support for our approximate model at strong coupling. One fermion is tightly bound and highly localized around the center of the trimer, while the other tends to be on the opposite side of the ring (we use periodic boundary conditions), albeit with much more freedom to move about the ring. In fact, due to the high degree of localization of the particle in the trimer, the separation of the two particles can be approximately regarded as the position of the free fermion.

TABLE III. Lattice sizes  $N_x$  used for each entry of Table II.

$\epsilon_B$	System					
	2 + 1 + 1	2 + 2 + 1	3 + 1 + 1	2 + 2 + 2	3 + 2 + 1	4 + 1 + 1
$10^{-3}$	41	15	15	15	15	15
$2 \times 10^{-3}$	41	15	15	15	15	15
$5 \times 10^{-3}$	41	15	15	15	15	15
$10^{-2}$	41	41	21	15	15	15
$2 \times 10^{-2}$	41	41	21	15	15	15
$5 \times 10^{-2}$	41	41	21	15	15	15
$7.5 \times 10^{-2}$	41	41	21	15	15	15
$10^{-1}$	41	41	21	15	15	15
$2 \times 10^{-1}$	41	41	21	15	15	15
$5 \times 10^{-1}$	41	41	25	15	21	21
$7.5 \times 10^{-1}$	41	41	51	31	21	31
1	41	41	51	31	21	31
1.5	41	41	51	31	21	31
2	41	41	51	31	25	31
3	41	41	51	31	31	31
5	41	41	61	31	31	31
7.5	41	41	61	41	41	41
10	41	41	61	41	41	41

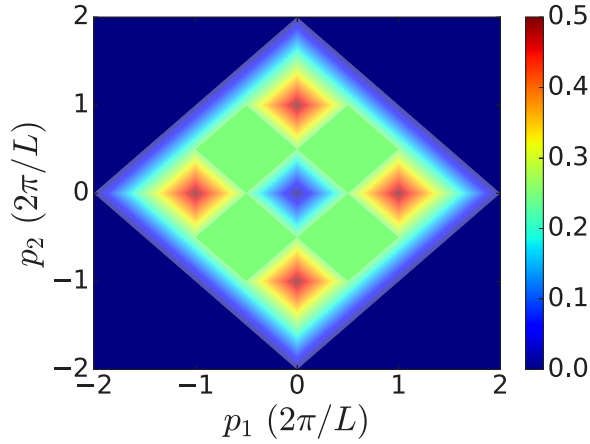


FIG. 3. Weakly interacting ( $\epsilon_B = 10^{-4}$ ) momentum density of two identical particles in the  $2 + 1 + 1$  system with the distinct particles integrated out. Here, identical particles fill the Fermi level rather than take on opposing momenta.

The roughly sinusoidal shape of this curve in Fig. 7 is thus yet another validation of our approximation at strong coupling.

#### D. Contact

Tan's contact [42–44] controls the high-momentum (short-distance) asymptotics of correlation functions in theories with short-range interactions. While the resulting universal relations have not yet been derived for the present case, it is easy to see using the Feynman-Hellmann theorem that the contact can be expressed as the derivative of the energy with respect to the logarithm of the scattering length (as shown for the system considered here in Ref. [29]). Here, we work in terms of the binding energy rather than the scattering length, such that the (dimensionless) contact takes the form

$$C = -4\pi \frac{\partial \mathcal{E}}{\partial (\ln \epsilon_B)}, \quad (16)$$

where  $(2\pi/L)^2 \mathcal{E} = E$ . We compute this derivative from a cubic spline interpolation of the energy and present the re-

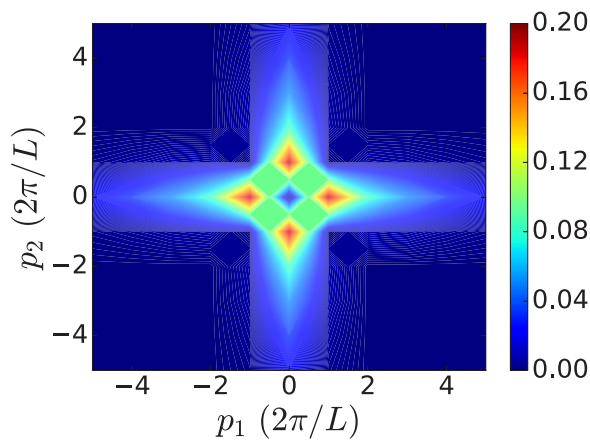


FIG. 4. Strongly interacting ( $\epsilon_B = 10$ ) momentum density of two identical particles in the  $2 + 1 + 1$  system with the distinct particles integrated out.

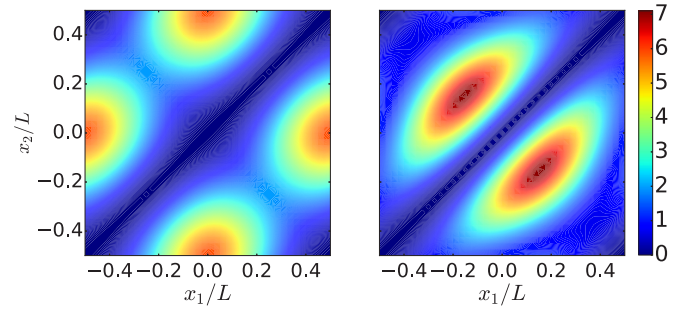


FIG. 5. Weakly interacting particle density (left:  $E - E_{FG} = -6\epsilon_B$ ; right:  $E - E_{FG} = -4\epsilon_B$ ) of two identical particles in the  $2 + 1 + 1$  system. For the two distinct particles, one is fixed at the origin and the other is integrated out.

sults in Fig. 8, where we divide by the number of whole trimers,  $\nu$ , that can be formed in each system. Though there are some small deviations (possibly stemming from the interpolation), the curves for all six cases overlap across the entire range of coupling values. The agreement is strongest at large coupling, indicating that the energy there is dominated by whole trimers—were there larger molecules forming, we would expect to see variation among the different systems. At intermediate coupling strengths, the modest differences may reflect competition between the different particles for inclusion in the trimer.

As mentioned above, the contact governs the short-distance behavior of theories with short-range interactions. We therefore expect the well-known host of universal relations (previously derived for two-body interactions) to have analogs for the present system. It is not difficult to see, following the derivations of Ref. [45], that the short-distance behavior of the  $N$ -particle wave function should obey

$$\psi(x_1, x_2, \dots, x_N) \rightarrow \ln(r_{ijk} \sqrt{\epsilon_B}) A_{ijk}(R_{ijk}, \theta_{ijk}, \{x_q\}) + O(r_{ijk}), \quad (17)$$

where  $\{x_q\} = (x_q)_{q \neq i, j, k}$ ;  $\mathbf{r}_{ijk} = (x_i - x_j, x_i - x_k)$ , such that  $(r_{ijk}, \theta_{ijk})$  is its polar representation (and therefore  $r_{ijk}$  is

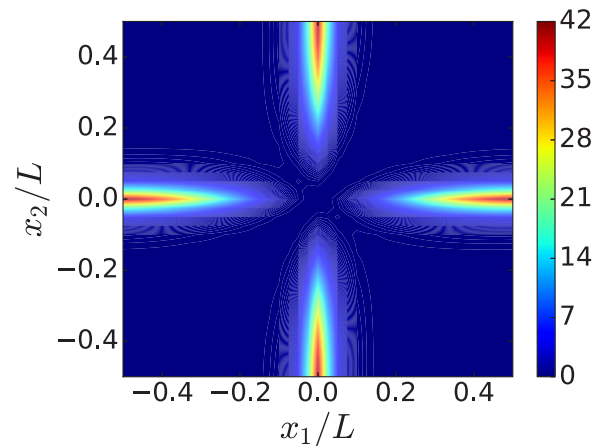


FIG. 6. Strongly interacting ( $\epsilon_B = 10$ ) particle density of two identical particles in the  $2 + 1 + 1$  system. For the two distinct particles, one is fixed at the origin and the other is integrated out.

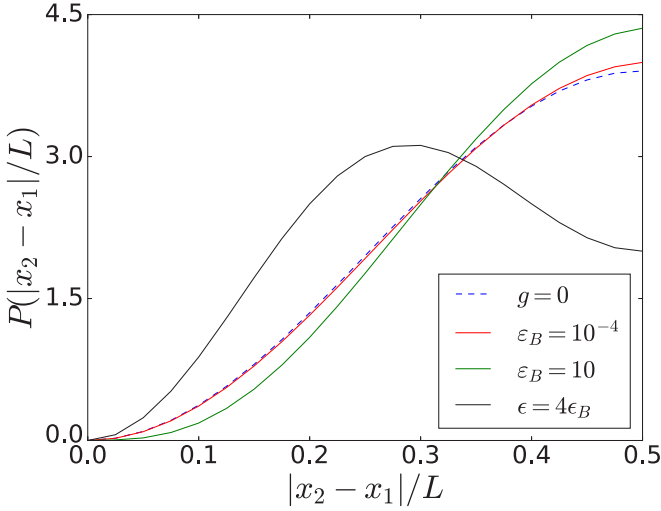


FIG. 7. Probability  $P(|x_2 - x_1|/L)$  of finding the two identical particles at a given separation  $|x_2 - x_1|$  of the two identical particles in the 2+1+1 problem. This function is translation invariant after integrating over all positions of the two distinct particles as in Eq. (15). The stronger the interaction, the farther apart the particles are likely to be.

a measure of the distance between particles  $i, j, k$ , where each index corresponds to a different particle species);  $R_{ijk} = (x_i + x_j + x_k)/3$  is the center-of-mass coordinate of particles  $i, j, k$ ; and  $A_{ijk}$  is the regular part of the wave function. As mentioned above, this form is expected at short distances (as a result of the short-range behavior of the three-body problem), which here means  $r_{ijk}\sqrt{\epsilon_B} \ll 1$ .

While we defer a more complete account and derivation of universal relations to future work, we point out here for completeness how such calculations would proceed in the particular case of the trimer distribution function, which is

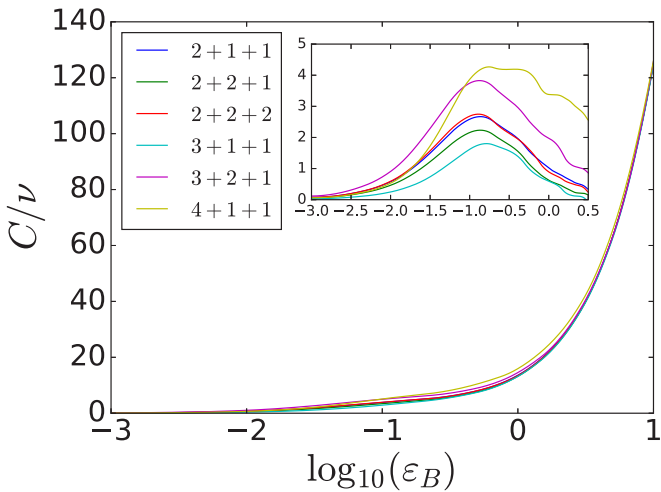


FIG. 8. Tan’s contact divided by the number of trimers present,  $\nu$ , as a function of the dimensionless trimer binding energy  $\epsilon_B$ . (Inset) Same as main plot, after subtracting the contact for  $\nu$  trimers; the oscillations at strong coupling are due to interpolation effects on the energy upon numerical differentiation.

defined as

$$g_{123}^{(3)}(R, \mathbf{r}) = \int dx_1 \dots dx_N |\psi(x_1, x_2, \dots, x_N)|^2 \times \sum_{i_1, i_2, i_3}^{N_1, N_2, N_3} \delta(x_{i_1} - f_1) \delta(x_{i_2} - f_2) \delta(x_{i_3} - f_3), \quad (18)$$

where  $i_1, i_2, i_3$  correspond to the three different species,  $f_1 = R + (r_1 + r_2)/3$ ,  $f_2 = f_1 - r_1$ ,  $f_3 = f_1 - r_2$ , and  $\mathbf{r} = (r_1, r_2)$ . The first step is to insert Eq. (17) into the above expression for  $g_{123}^{(3)}(R, \mathbf{r})$ , when  $r = |\mathbf{r}| \rightarrow 0$ . Then, each term in  $g_{123}^{(3)}(R, \mathbf{r})$  is governed by the divergent piece of the wave function, which is the same for all terms, such that,

$$g_{123}^{(3)}(R, \mathbf{r}) \rightarrow \ln^2(r\sqrt{\epsilon_B}) F(R, \theta), \quad (19)$$

where

$$F(R, \theta) = \sum_{i_1, i_2, i_3}^{N_1, N_2, N_3} \int \prod_{k \neq i_1, i_2, i_3} dx_k |A_{i_1, i_2, i_3}(R, \theta, \{x_q\})|^2, \quad (20)$$

where  $\{x_q\} = (x_q)_{q \neq i, j, k}$ . Finally, by integrating over  $R$  and  $\theta$ , we obtain the integrated trimer distribution function  $G_{123}^{(3)}(r)$ , which inherits the short-distance behavior of  $g_{123}^{(3)}$ , i.e.,

$$G_{123}^{(3)}(r) \equiv \int dR d\theta g_{123}^{(3)}(R, \mathbf{r}) \rightarrow \ln^2(r\sqrt{\epsilon_B}) \mathcal{K}. \quad (21)$$

Here, the constant  $\mathcal{K}$  is determined by the contact, up to a coupling-independent factor. Following the derivations of Ref. [45], it is not difficult to see that our use of the Feynman-Hellmann theorem to access the contact [i.e., the adiabatic relation of Eq. (16)] can also be derived starting from Eq. (17) by evaluating the expectation value of the Hamiltonian. As above, the crucial aspect of the derivation is that  $\sqrt{\epsilon_B}$  sets the scale for the short-distance behavior, such that once the divergent piece has been factored out, what remains is proportional to the integrated regular part squared  $|A_{i_1, i_2, i_3}(R, \theta, \{x_q\})|^2$ . One can glean from the above example that the universal relations of the 1D system explored here will always mimic those of the 2D analog with two-body interactions.

## V. SUMMARY AND CONCLUSIONS

To summarize, we have extended the analysis of the three-body problem with a three-body contact interaction of Ref. [29] beyond the 1 + 1 + 1 system. Here, we have studied the higher-body problems up to six particles in all possible nontrivial combinations, namely, four particles (2 + 1 + 1); five particles (2 + 2 + 1 and 3 + 1 + 1); and six particles (2 + 2 + 2, 3 + 2 + 1, and 4 + 1 + 1). With the exception of the 2 + 2 + 2 case, which will form two trimers, each of the cases considered will form only one trimer. To solve those problems, we designed a self-consistent numerical approach which is the natural generalization of the analytic solution of the 1 + 1 + 1 problem of Ref. [29]. Our solution gives immediate access to essential properties such as the energy and Tan’s contact, but it also provides the multiparticle wave function, from which everything else is calculable.

As a function of the interaction strength, our results show that the energy of the various systems studied presents clear variations as a function of the system composition (see Fig. 1). On the other hand, we have found that Tan's contact displays extremely small variations across the different systems. At weak coupling, we compare with first-order perturbation theory in the bare coupling, renormalized using the three-body binding energy, and find good agreement after taking into account the breaking of the degeneracy of noninteracting ground states, i.e., using degenerate perturbation theory. At strong coupling, one expects a description dominated by bound trimers plus noninteracting particles. We implemented that approximation by representing the trimer as a pointlike fermion of mass  $3m$  interacting with the remaining particles via a hard-core potential, which we implemented simply as a vanishing boundary condition in the many-body wave function (à la Bethe-Peierls). That description works remarkably well already at couplings of  $\varepsilon_B = 10$ , as shown in Fig. 1.

Our calculations suggest that, as in the case of pure two-body contact forces, Pauli exclusion provides a strong repulsion that overpowers any residual attraction coming from

the three-body force. The trimers always experience a repulsive interaction, as far as we have explored. The emerging picture is therefore that of a crossover between the original, attractively interacting fermions (weakly bound into extended trimers) and deeply bound composite fermions (strongly localized trimers) with a residual repulsive interaction. Although we have not found trimer-trimer binding, it would be interesting to investigate the effect of a finite interaction range, which has been shown to yield droplet formation and eventually lead to a liquid-gas transition in 1D systems with finite-range, two-body interactions (see, e.g., [46,47]).

In addition to a numerical calculation of the contact, we have also outlined the derivation of the universal behavior of correlation functions at short distances. A more complete derivation is left for future work, but the general procedure and how it differs from the two-body interaction case is clear: two-body quantities are replaced by three-body quantities, and the two-particle short-distance limit is replaced by the trimer short-distance limit. Thus, we expect that all the known universal relations controlled by the contact can be generalized to the present system by a simple modification of the known derivations.

- 
- [1] *The BCS-BEC Crossover and the Unitary Fermi Gas*, edited by W. Zwerger (Springer, Berlin, 2012).
- [2] G. C. Strinati, P. Pieri, G. Röpke, P. Schuck, and M. Urban, *Phys. Rep.* **738**, 1 (2018).
- [3] Y. Nishida and D. T. Son, *Phys. Rev. D* **76**, 086004 (2007).
- [4] P. Carruthers, *Phys. Rev. D* **2**, 2265 (1970).
- [5] R. Jackiw, *Phys. Today* **25**, 23 (1972).
- [6] R. Jackiw, in *M.A.B. Beg Memorial Volume*, edited by A. Ali and P. Hoodbhoy (World Scientific, Singapore, 1991), pp. 1–16.
- [7] B. R. Holstein, *Am. J. Phys.* **61**, 142 (1993).
- [8] K. Martiyanov, V. Makhlov, and A. Turlapov, *Phys. Rev. Lett.* **105**, 030404 (2010).
- [9] B. Fröhlich, M. Feld, E. Vogt, M. Koschorreck, W. Zwerger, and M. Köhl, *Phys. Rev. Lett.* **106**, 105301 (2011).
- [10] Y. Zhang, W. Ong, I. Arakelyan, and J. E. Thomas, *Phys. Rev. Lett.* **108**, 235302 (2012).
- [11] A. A. Orel, P. Dyke, M. Delehay, C. J. Vale, and H. Hu, *New J. Phys.* **13**, 113032 (2011).
- [12] E. Vogt, M. Feld, B. Fröhlich, D. Pertot, M. Koschorreck, and M. Köhl, *Phys. Rev. Lett.* **108**, 070404 (2012).
- [13] B. Fröhlich, M. Feld, E. Vogt, M. Koschorreck, M. Köhl, C. Berthod, and T. Giamarchi, *Phys. Rev. Lett.* **109**, 130403 (2012).
- [14] V. Makhlov, K. Martiyanov, and A. Turlapov, *Phys. Rev. Lett.* **112**, 045301 (2014).
- [15] W. Ong, C. Cheng, I. Arakelyan, and J. E. Thomas, *Phys. Rev. Lett.* **114**, 110403 (2015).
- [16] M. G. Ries, A. N. Wenz, G. Zürn, L. Bayha, I. Boettcher, D. Kedar, P. A. Murthy, M. Neidig, T. Lompe, and S. Jochim, *Phys. Rev. Lett.* **114**, 230401 (2015).
- [17] P. A. Murthy, I. Boettcher, L. Bayha, M. Holzmann, D. Kedar, M. Neidig, M. G. Ries, A. N. Wenz, G. Zürn, and S. Jochim, *Phys. Rev. Lett.* **115**, 010401 (2015).
- [18] K. Fenech, P. Dyke, T. Pepler, M. G. Lingham, S. Hoinka, H. Hu, and C. J. Vale, *Phys. Rev. Lett.* **116**, 045302 (2016).
- [19] L. P. Pitaevskii and A. Rosch, *Phys. Rev. A* **55**, R853 (1997).
- [20] E. Taylor and M. Randeria, *Phys. Rev. Lett.* **109**, 135301 (2012).
- [21] G. Bertaino and S. Giorgini, *Phys. Rev. Lett.* **106**, 110403 (2011).
- [22] J. Hofmann, *Phys. Rev. Lett.* **108**, 185303 (2012).
- [23] C. Chafin and T. Schäfer, *Phys. Rev. A* **88**, 043636 (2013).
- [24] H. Shi, S. Chiesa, and S. Zhang, *Phys. Rev. A* **92**, 033603 (2015).
- [25] E. R. Anderson and J. E. Drut, *Phys. Rev. Lett.* **115**, 115301 (2015).
- [26] C. R. Ordóñez, *Phys. A (Amsterdam, Neth.)* **446**, 64 (2016).
- [27] W. Daza, J. E. Drut, C. Lin, and C. Ordóñez, *Phys. Rev. A* **97**, 033630 (2018).
- [28] J. Levensen and M. M. Parish, *Annu. Rev. Cold At. Mol.* **5**, 1 (2015).
- [29] J. E. Drut, J. R. McKenney, W. S. Daza, C. L. Lin, and C. R. Ordóñez, *Phys. Rev. Lett.* **120**, 243002 (2018).
- [30] Y. Nishida, *Phys. Rev. A* **97**, 061603 (2018).
- [31] L. Pricoupenko, *Phys. Rev. A* **97**, 061604 (2018).
- [32] G. Guijarro, A. Pricoupenko, G. E. Astrakharchik, J. Boronat, and D. S. Petrov, *Phys. Rev. A* **97**, 061605 (2018).
- [33] Y. Sekino and Y. Nishida, *Phys. Rev. A* **97**, 011602 (2018).
- [34] H.-W. Hammer, A. Nogga, and A. Schwenk, *Rev. Mod. Phys.* **85**, 197 (2013).
- [35] M. A. Cazalilla and A. M. Rey, *Rep. Prog. Phys.* **77**, 124401 (2014).
- [36] T. B. Ottenstein, T. Lompe, M. Kohnen, A. N. Wenz, and S. Jochim, *Phys. Rev. Lett.* **101**, 203202 (2008).
- [37] A. Modawi and A. Leggett, *J. Low Temp. Phys.* **109**, 625 (1997).

- [38] J. R. Williams, E. L. Hazlett, J. H. Huckans, R. W. Stites, Y. Zhang, and K. M. O'Hara, *Phys. Rev. Lett.* **103**, 130404 (2009).
- [39] L. Faddeev, *Sov. Phys. JETP* **12**, 1014 (1961).
- [40] G. Skorniakov and K. Ter-Martirosian, *Sov. Phys. JETP* **4**, 648 (1957).
- [41] J. J. Sakurai, *Modern Quantum Mechanics*, rev. ed. (Addison-Wesley, Reading, MA, 1994).
- [42] S. Tan, *Ann. Phys.* **323**, 2952 (2008).
- [43] S. Tan, *Ann. Phys.* **323**, 2971 (2008).
- [44] S. Tan, *Ann. Phys.* **323**, 2987 (2008).
- [45] F. Werner and Y. Castin, *Phys. Rev. A* **86**, 013626 (2012).
- [46] K. T. Law and D. E. Feldman, *Phys. Rev. Lett.* **101**, 096401 (2008).
- [47] V. V. Vyborova, O. Lychkovskiy, and A. N. Rubtsov, *Phys. Rev. B* **98**, 235407 (2018).